# Coexistence of an antiferromagnetically coupled dimer and isolated paramagnetic spin in 4-azaindol-2-yl nitronyl nitroxide crystal†

**Hideaki Nagashima, Noriko Hashimoto, Hidenari Inoue and Naoki Yoshioka***

*Department of Applied Chemistry, Faculty of Science and Technology, Keio University, Kohoku-ku, Yokohama 223-8522, Japan. E-mail: yoshioka@applc.keio.ac.jp*

***Received (in Montpellier, France) 4th November 2002, Accepted 22nd January 2003***
***First published as an Advance Article on the web 9th April 2003***



A novel stable organic radical, 2-(4-azaindol-2-yl)-4,4,5,5-tetramethyl-4,5-dihydro-1*H*-imidazoline-1-oxyl-3-oxide (**2**) was synthesized and its magneto-structural correlation is discussed. **2** crystallizes in the space group $C2/c$ with hydrogen bonding between two independent molecules (A and B) having different dihedral angles between the azaindole rings and nitronyl nitroxide units in the asymmetric unit. The molecules are further linked together with axisymmetrically related molecules (A* and B*) through hydrogen bonds (A-B* and A*-B) and π stacking (A-A*). The temperature dependence of the magnetic susceptibility reveals that half of the radicals are antiferromagnetically coupled as a dimer (singlet-triplet energy gap: $2J = -64$ cm$^{-1}$) while the other half behaves as an isolated monomer. DFT calculations (UB3LYP/6–31G*) of the dimeric coordinates extracted from the X-ray analysis rationalize the fact that the π-stacked A-A* dimer contributes to the antiferromagnetic coupling by a close contact between nitronyl nitroxide units.

## Introduction

Magnetism had been recognized as a unique characteristic of inorganic compounds such as metals and metal oxides. In the last decade, however, strenuous efforts have been made to create magnets that are composed of molecules.[1] Since the discovery of the first purely organic ferromagnet, *p*-nitrophenyl nitronyl nitroxide exhibiting a ferromagnetic phase transition at 0.60 K in 1991,[2] tens of organic ferromagnets with various chemical structures have been reported. In particular, tetramethyladamantane dinitroxyl, exhibiting a ferromagnetic phase transition at $T_c = 1.48$ K,[3] and dithiadiazolyl radical, exhibiting a canted ferromagnetism at $T_c = 36$ K, [4] are well-known as milestones in this field of organic radical magnetic materials. Because bulk magnetic ordering is closely correlated with the crystal structure (that is, the arrangement of open-shell molecules in the crystal), supramolecular design techniques, in which intermolecular interactions such as hydrogen bonding and other weak interactions are applied to realize a specific functionality,[5] have been introduced to the field of molecular magnetism to construct supramolecular spin networks. As successful examples, dihydroxyphenyl,[6] triazolyl,[7] and pyrimidinyl[8] nitronyl nitroxide derivatives have been reported to exhibit ferromagnetic interactions or ferromagnetic ordering in the low temperature region.

We have already reported that benzimidazol-2-yl nitronyl nitroxide (**1**) forms a hydrogen-bonded 1-D chain structure accompanying a close contact between magnetic orbitals in its crystal.[9] **1** shows an intermolecular ferromagnetic interaction, which can be reproduced by a 1-D Heisenberg ferromagnetic chain model with $J = +12$ cm$^{-1}$. For **1**, various hydrogen-bonding motifs had been expected by the combination of proton acceptor sites (two nitroxide O atoms and one imine N atom) and a proton donor site (NH proton). In the crystal exhibiting ferromagnetic interaction, however, one of the nitroxide O atom forms a branched hydrogen bond between NH sites in its own and neighboring molecules (Fig. 1). Another O atom at which the α spin is induced does not contribute to form hydrogen bonds and approaches the $sp^2$ C atom of a neighboring molecule at which β spin is polarized. This contact is repeated to form a hydrogen-bonded chain structure. Each chain is well isolated due to the steric effects of the benzimidazole ring and four methyl groups. The low dimensional magnetism is rationally explained by

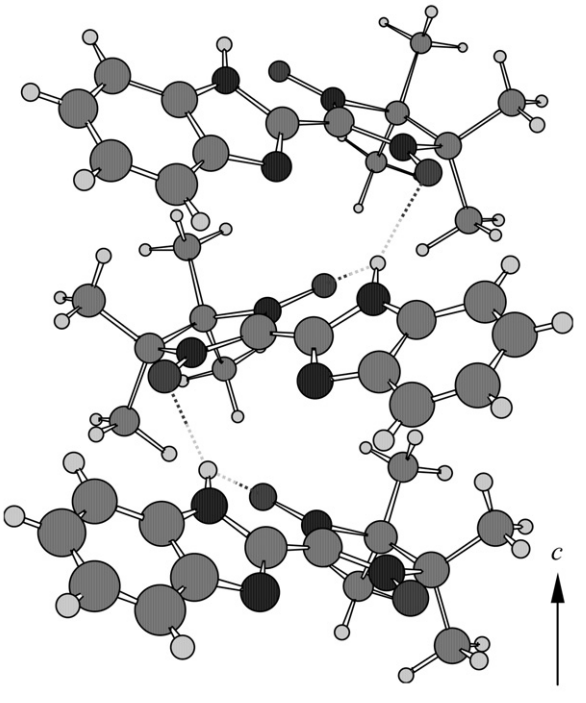


**Fig. 1** Hydrogen-bonded chain structure of **1** along the *c* axis.

† Electronic supplementary information available: final atomic positions, calculated atomic spin population, calculated optimized structure of **2** and the dimeric structures used to calculate *J*. See http://www.rsc.org/suppdata/nj/b2/b210820h/

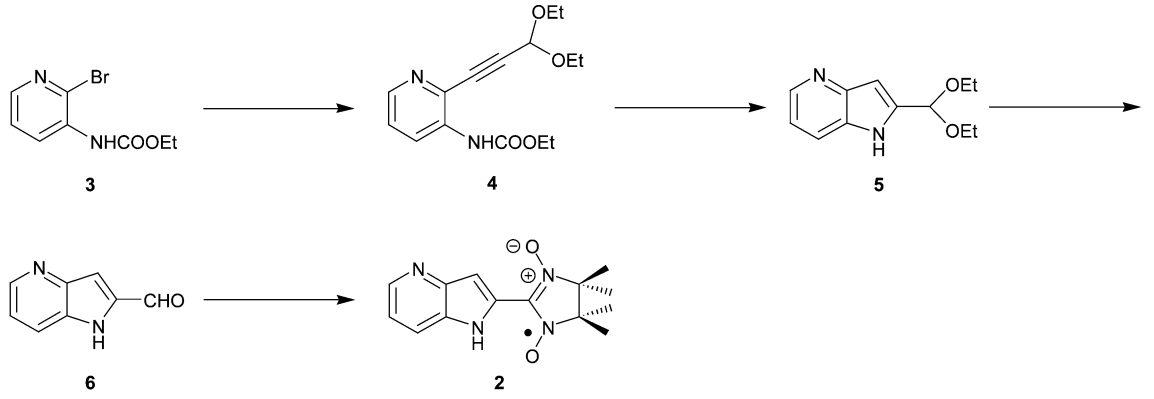


**Scheme 1** Synthetic route to **2**.



McConnell's I mechanism along the π-stacked direction.[10] We have been designing and characterizing a series of analogous derivatives of **1** to accumulate fundamental magneto-structural correlation data and to evaluate the use of the NHCC(NO)NO moiety as a supramolecular synthon for propagating intermolecular magnetic interactions.

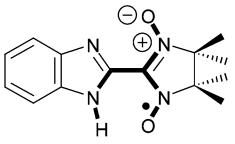

**1**

In the crystal of **1**, the imine N atom does not participate in the intermolecular hydrogen bond. The fact prompted us to synthesize a series of novel nitronyl nitroxide derivatives bearing azaindole rings, which are the structural isomers of the benzimidazole ring, that is a 3-azaindole bearing an imine N atom not in the five-membered ring but in the six-membered ring. Following this strategy, here we describe the synthesis of 4-azaindol-2-yl nitronyl nitroxide (**2**) and its magneto-structural correlation in the crystal.

## Results and discussion

### Synthesis

**2** was obtained by a 4-step synthesis described in Scheme 1, which is a modification of the procedure used for the preparation of unsubstituted 4-azaindole by Yamanaka *et al.*[11] Acetal **5**, which is easily converted to the corresponding aldehyde **6** by hydrolysis, was prepared by the Sonogashira cross coupling of ethyl bromopyridine carbamate **3** with propargylaldehyde diethylacetal using a palladium catalyst to yield **4**, followed by intramolecular cyclization of **4** under strong basic conditions using KO*t*Bu. The nitronyl nitroxide unit was introduced according to the procedure reported by Ullman *et al.*:[12] condensation of the corresponding aldehyde **6** with 2,3-bis (hydroxyamino)-2,3-dimethylbutane, followed by chemical oxidation with $NaIO_4$. A single crystal of **2** suitable for X-ray diffraction analysis was prepared by slow evaporation from a methanol solution.

### Spin density distribution

The EPR spectrum of a $3 \times 10^{-5}$M benzene solution of **2** at room temperature is shown in Fig. 2. The spectrum consists of five main lines with relative intensities of 1:2:3:2:1, due to the coupling of the unpaired electron with two equivalent nitrogen nuclei ($I = 1$) of the nitronyl nitroxide unit. The spectrum was further resolved to a more complex pattern, implying the coupling of the unpaired electron to twelve hydrogen nuclei ($I = 1/2$) of the four methyl groups and hydrogen and/or nitrogen nuclei of the 4-azaindole ring. The hyperfine coupling constants (hfccs) obtained by non-linear curve fitting of the spectrum[13] are summarized in Table 1. The hfcc for the 3H proton of the 4-azaindole ring is larger than that observed for other protons, and the value is close to that observed for *ortho* protons in phenyl nitronyl nitroxide derivatives.[14] A moderate amount of spin density was also observed on the N atom at the 4 position of the azaindole ring although the N atom is removed from the nitroxide spin center.

Hfccs were calculated with density functional theory using Gaussian 98.[15] UB3LYP[16]/EPR-II[17] level single-point calculations on the UB3LYP/cc-pVDZ[18] optimized structure of **2** [Fig. S1, see Electronic supplementary information (ESI)] were carried out to keep up with the recent trend to estimate reliable hfccs.[14] Calculated hfccs are compared with experimental ones in Table 1 and computed atomic spin densities are summarized

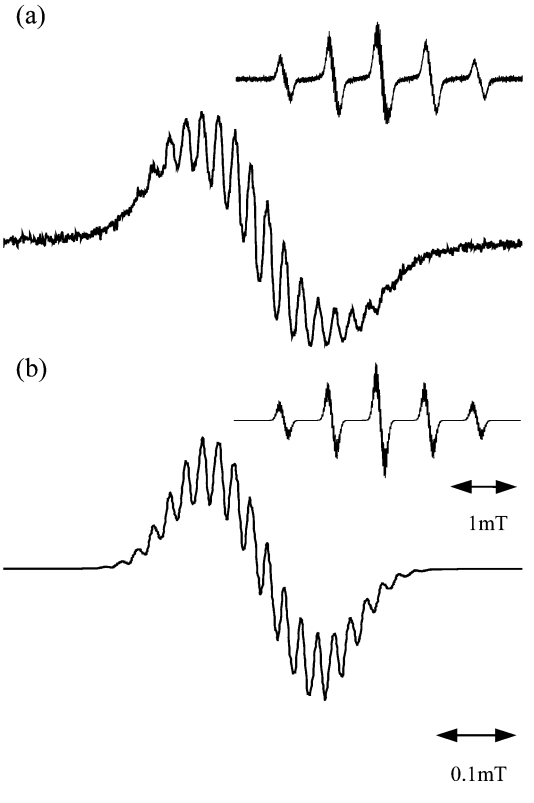


**Fig. 2** Experimental (a) and simulated (b) EPR spectra of **2**. The main figures correspond to the central signals ($M_I = 0$).

**Table 1** Experimental and calculated hfccs of **2**

| Site | Exptal hfccs[a] /mT | Calcd hfccs[b] /mT |
|---|---|---|
| $a_N$, nitroxide N | 0.731 | (+)0.597, (+)0.529 |
| $a_N$, 4-azaindole 1,4 N | 0.043, 0.016 | (−)0.023, (−)0.021 |
| $a_H$, methyl H | 0.021 | – |
| $a_H$, 4-azaindole 3 H | 0.040 | (+)0.178 |
| $a_H$, 4-azaindole 1,5,6,7 H | 0.018, 0.014 | (+)0.018, (−)0.005 |
| | 0.011, 0.004 | (+)0.061, (−)0.014 |

[a] In $3 \times 10^{-5}$M benzene solution at room temperature. [b] UB3LYP/EPR-II//UB3LYP/cc-pVDZ.

in Table S1 (see ESI). Experimental and calculated results suggest that small spin densities are located on the methyl groups and azaindole ring, though most of the spin density is localized on the ONCNO moiety; the close contact through the azaindole unit might contribute to the observed magnetic interaction.

## Crystal structure

Crystallographic data and the final positional parameters of **2** are summarized in Tables 2 and S2 (see ESI), respectively. **2** crystallizes in the space group $C2/c$ with two independent molecules (A and B) in the asymmetric unit, containing 16 independent molecules in one unit cell. Fig. 3 shows ORTEP drawings of molecules A and B. The dihedral angles between the best planes of the pyrrole rings and the ONCNO moieties are 3.3° and 5.8° for A and B, respectively. Both the geometries have high coplanarity when compared to the corresponding angle of 24.3° between the imidazole ring and ONCNO moiety in **1**. This is because of the intramolecular hydrogen bonds C–H···O–N and N–H···O–N. Fig. 4 shows the crystal packing of **2**. Molecules A and B are linked together through the N(5)···O(22) hydrogen bond whose distance is 3.02 Å. The dimer is further linked together by an axisymmetrically related pair (symmetry code: $-x+2$, $y$, $-z+1/2$; A* and B*). A and B* (or A* and B) are also linked through a hydrogen bond, N(25)*···N(6) [or N(25)···N(6)*]; the distance is 3.02 Å. Though the imine N atom does not participate in the intermolecular hydrogen bond in **1**, it does in the crystal of **2**. In addition, A and A* are π-stacked to give a noticeable dimeric structure. In the π-stacked dimer A-A*, close contact between nitroxide moieties is observed; the distances between O(21)···O(21)* and N(21)···O(23)* [or O(23)···N(21)*] are 3.70 and 3.58 Å, respectively. Four molecules, A, A*, B and B*, are assembled through hydrogen bonds and π-stacking with the assembly extending in the *ab* plane. Focusing on the

**Table 2** Crystal and refinement data of **2**

| | |
|---|---|
| Chemical formula | $C_{14}H_{17}N_4O_2$ |
| Formula weight | 273.31 |
| Crystal system | Monoclinic |
| Space group | $C2/c$ (No.15) |
| $a$/Å | 19.426(2) |
| $b$/Å | 14.881(3) |
| $c$/Å | 21.824(2) |
| $\beta$/° | 116.880(7) |
| $U$/Å$^3$ | 5627.3(13) |
| $Z$ | 16 |
| $T$/K | 297 |
| $\mu$/mm$^{-1}$ | 0.090 |
| Total reflections | 7361 |
| Unique reflections | 6454 |
| Reflections used | 4365 |
| $R_{int}$ | 0.0156 |
| $R = \Sigma(\|\|F_o\| - \|F_c\|\|)/\Sigma\|F_o\|$ | 0.0492 |
| $R_w = [\Sigma[w(F_o^2 - F_c^2)^2]/\Sigma w(F_o^2)^2]^{1/2}$ | 0.1667 |

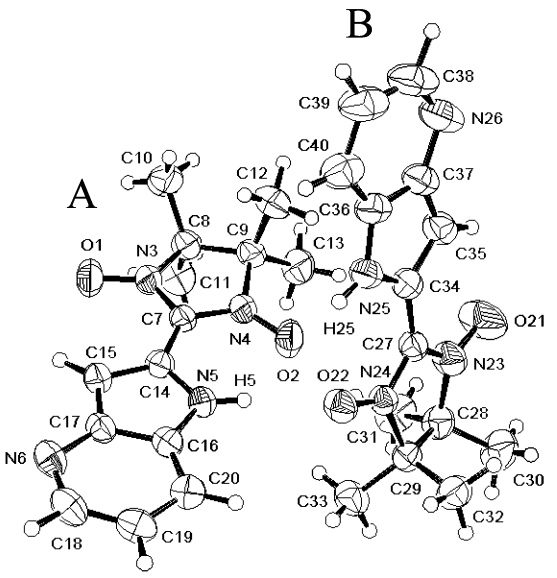


**Fig. 3** ORTEP drawing and atomic numbering of the molecular structures of **2**.

π-stacked dimer, A-A* is surrounded by six molecules: B, B*, B**, B***, B****and B***** in the *ab* plane (symmetry codes: * $-x+2$, $y$, $-z+1/2$; ** $x+1/2$, $y-1/2$, $z$; *** $-x+3/2$, $y+1/2$, $-z+1/2$; **** $x+1/2$, $y+1/2$, $z$; ***** $-x+3/2$, $y-1/2$, $-z+1/2$). The A-A* dimers are isolated from each other.

## Solid-state magnetic measurement

The temperature dependence of the magnetic susceptibility was measured for a polycrystalline sample of **2** with a SQUID susceptometer in the temperature range of 1.8–300 K under an applied field of 0.5 T. The diamagnetic contribution was estimated using Pacault's method.[19] Fig. 5 (inset) shows the $\chi_m T$ *vs.* $T$ plot where $\chi_m$ is the molar magnetic susceptibility and $T$ is the absolute temperature. At 300 K $\chi_m T$ is equal to 0.34 emu·K·mol$^{-1}$, a little less than what would be expected for an isolated monoradical (0.38 emu·K·mol$^{-1}$). The value decreases with decreasing temperature down to *ca.* 10 K, and becomes nearly constant (0.18 emu·K·mol$^{-1}$) below this temperature, corresponding to half the value expected for an isolated monoradical (0.19 emu·K·mol$^{-1}$). These results suggest the existence of two magnetic sub-lattices, in which the radicals are magnetically independent or interact antiferromagnetically.

In order to clarify the magnetic interaction, the paramagnetic component was subtracted from the experimental Curie plot as shown in Fig. 5. The residual component has a broad maximum at *ca.* 50 K and approaches 0 emu·K·mol$^{-1}$ as temperature is lowered, suggesting a low-dimensional antiferromagnetic system. The magnetic data can be nicely fit to a combined model with the Bleaney–Bowers expression[20] and Curie's law as described in eqn. (1):

$$\chi_m = f \times \left[0.5 \times \frac{C}{T} + 0.5 \times \frac{N_A g^2 \mu_B^2}{k_B T} \frac{1}{3 + \exp(-2J/k_B T)}\right] \quad (1)$$

A correlation factor $f$ was employed to the experimental error for Curie constant $C$ (= 0.375 emu K mol$^{-1}$) for an isolated doublet state. The best-fit parameters are $f = 0.94$ and a singlet-triplet energy gap of $2J = -64$ cm$^{-1}$.

## Magneto-structural correlation

In order to specify the magnetic interaction pathways, density functional calculations for three different dimeric coordinates

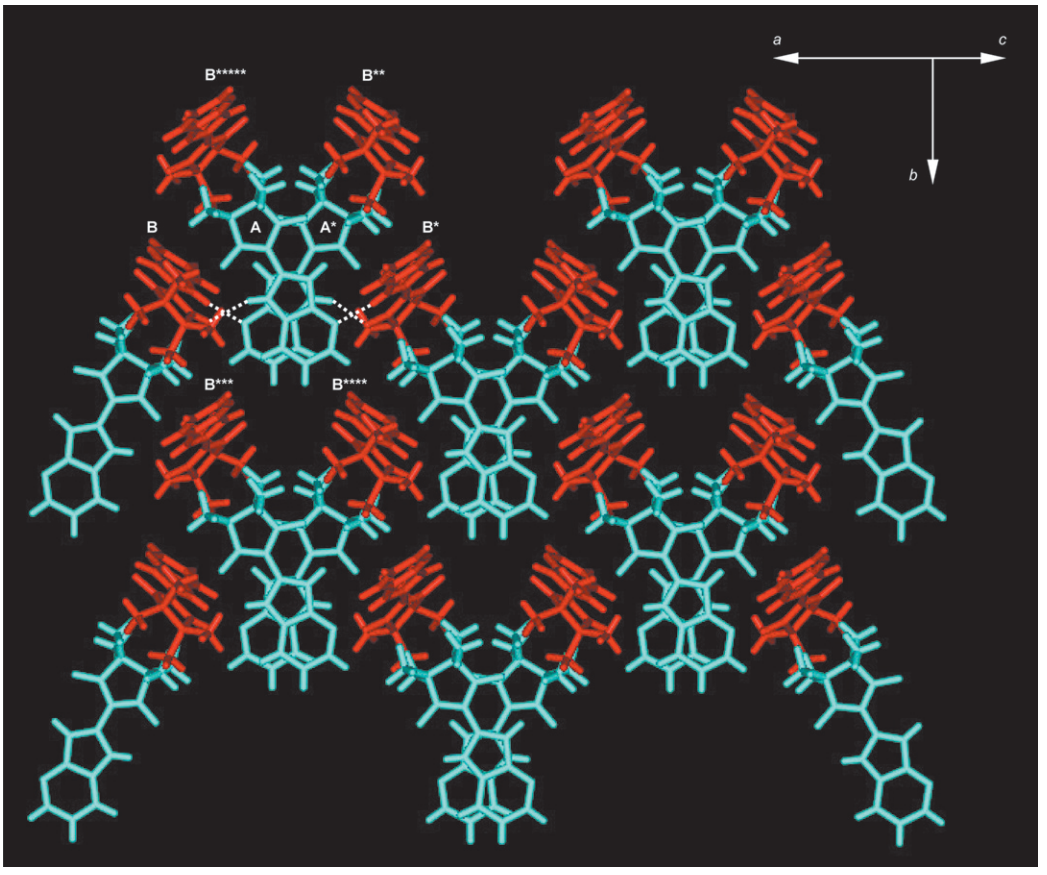


**Fig. 4** Crystal packing of **2** projected onto the *ab* plane. Molecules A and B are colored blue and red, respectively.



extracted from the X-ray analysis were carried out. Selected dimeric coordinates [A-B, A-A* and A-B* (or A*-B)] are illustrated in Fig. S2 (see ESI). The calculations were carried out using Gaussian 98.[15] Tight convergence was used to discuss small energy differences ($10^{-8}$ a.u.). HOMO-LUMO mixed initial guesses were created to estimate broken-symmetry singlet state energies. $J$ values were calculated at the UB3LYP/6-31G* level using eqn. (2) developed by Yamaguchi *et al.*[21]

$$J = \frac{E^{LS} - E^{HS}}{\langle S^2 \rangle^{HS} - \langle S^2 \rangle^{LS}} \quad (2)$$

Calculation of the A-A* dimer found a singlet ground state with $J = -25.1$ cm$^{-1}$, giving good agreement with that obtained from experimental results ($J = -32$ cm$^{-1}$). The calculation supports the discussion that the magnetic interaction expected from the correlation between the crystal structure and spin density distribution is reasonable. Calculations for A-B and A-B* (or A*-B) dimers, on the other hand, found $J = \pm 0.0$ cm$^{-1}$ for both the dimers, showing that these contacts do not contribute to the magnetic character. Even though small spin densities were observed at the N and H atoms of the 4-azaindole unit from the solution EPR spectrum and the result is supported by the DFT calculation, the densities were probably too small to affect the solid-state magnetic measurements.

A quite similar magnetic behavior has been reported for 2-(3′,5′-difluorophenyl)nitronyl nitroxide (**7**).[22,23] In the crystal, two crystallographically independent molecules formed a pair of dimers, in one of which a close N···O contact of 3.97 Å of the nitronyl nitroxide units was found. Its $\chi_m T$ value also reached half the value of the isolated monoradical as temperature was lowered, showing that half of the spins interact antiferromagnetically with $2J = -15$ cm$^{-1}$. Lahti *et al.* rationalized that close contacts between the NO groups in the A dimers in reference 23 dominated the magnetic behavior.

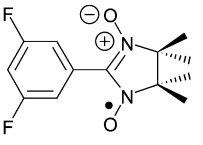


**7**

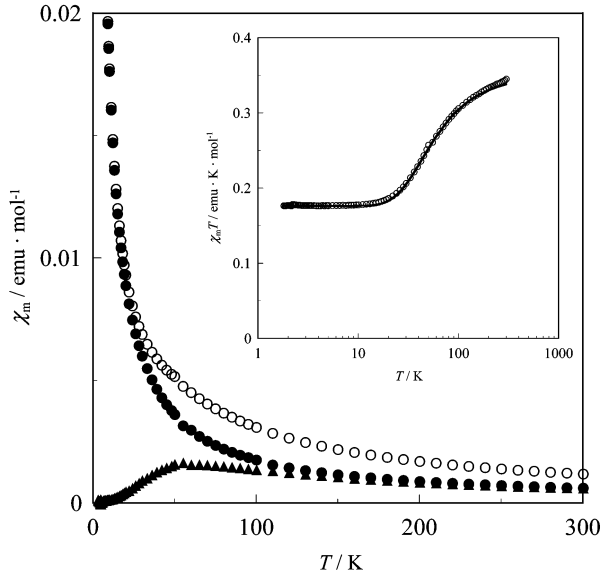


**Fig. 5** Temperature dependence of $\chi_m$ of **2**(○) and its deconvolution into paramagnetic(●) and antiferromagnetic(▲) components. The inset shows the temperature dependence of $\chi_m T$. The solid line corresponds to the calculated curve using eqn. (1) (see text).

Let us consider the magnetic coupling mechanism of **2**. According to the DFT calculations mentioned above, α spin densities are induced on the N and O atoms of the nitronyl nitroxide unit. The close contact between atoms on which spin densities of the same sign are induced causes an antiferromagnetic interaction according to McConnell's I mechanism.[10] When this mechanism is applied to the N(21)···O(23)* [or O(23)···N(21)*] contact observed in the A-A* dimer, an antiferromagnetic interaction seems plausible. But the magnitude of the magnetic interaction, $2J = -64$ cm$^{-1}$ for **2**, is smaller than that expected from the N···O distance of 3.58 Å of the nitronyl nitroxide units when compared to 2-(imidazol-2-yl)-nitronyl nitroxide (**8**) for which $2J = -123$ cm$^{-1}$ and the separation is 3.41 Å:[9a] $2J$ for **2** has only half the value found for **8**. In the magnetically interacting dimer observed in the crystal of **8**, π-stacking between imidazole units was not found; instead radical units approached in a head-to-head fashion. In the A-A* dimer observed in the crystal of **2**, on the other hand, the axis of symmetry enables 4-azaindole units to π-stack as well as the nitronyl nitroxide units. The spin density population on 2-C and 3-C of the 4-azaindole unit at the UB3LYP/EPR-II//UB3LYP/cc-pVDZ level were +0.042 and −0.072, respectively (Table S1, see ESI). The closest contact between the 4-azaindole unit was between two C atoms [C(14)···C(15)* or C(14)*···C(15); 3.58 Å], on which spin densities of different signs were induced; thus, a ferromagnetic interaction was expected when taking into account this contact. To estimate the contribution of the π-stacking observed in the A-A* dimer to the magnetic character of **2**, we also carried out DFT calculations for simplified ONCNO dimers of **2** and **8**[9c] Calculated $J$ values for the simplified dimers of **2** and **8** are −21.3 and −21.4 cm$^{-1}$, respectively, almost the same. On the other hand, calculated $J$ values for the full dimers are −25.1 and −38.6 cm$^{-1}$,[9c] respectively, qualitatively reproducing the difference between the experimentally obtained $J$ values of **2** and **8**. These computational results support the notion that the magnetic interaction through induced spin density on the 4-azaindole unit contributes to weaken the antiferromagnetic interaction of the A-A* dimer.

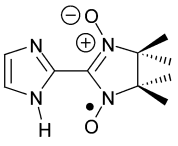

**8**

## Summary

The magnetic properties of **2** were clearly explained by taking into account its crystal structure and the spin density distribution within the molecule. Even though three major dimeric structures [A-B, A-B* (A*-B) and A-A*] were found in the crystal, only the A-A* dimer contributes to the magnetic character. The close contact between nitronyl nitroxide units within the A-A* dimer causes a strong antiferromagnetic interaction, which can be explained by applying McConnell's I mechanism.

## Experimental

### General methods and materials

Magnetic susceptibility measurements were carried out using a Quantum Design MPMS-5 SQUID susceptometer working at a field strength of 0.5 T in the temperature range of 1.8–300 K. The ESR spectrum was recorded on a JEOL JES-RE3X X-band (9.4 GHz) spectrometer. $^1$H NMR spectra were obtained on a Varian MVX-300 spectrometer. Mass spectra were measured on a JEOL JMS-DX302 mass spectrometer using *m*-nitrobenzylalcohol as the matrix.

Ethyl 2-bromo-3-pyridinecarbamate (**3**)[11] and 2,3-bis(hydroxyamino)-2,3-dimethylbutane[24] were prepared as described previously. Other reagents were commercially available and used without further purification.

### Syntheses

**Ethyl 2-(3,3-diethoxypropynyl)-3-pyridinecarbamate (4).** To a solution of **3** (4.00 g, 16.3 mmol) and propargylaldehyde diethylacetal (3.14 g, 24.5 mmol) in triethylamine (80 cm$^3$) were added bis(triphenylphosphine)palladium(II) chloride (0.56 g, 0.8 mmol) and copper(I) iodide (0.28 g, 1.5 mmol). The mixture was stirred at 100 °C under nitrogen for 5 h, after which the solvent was removed under reduced pressure. The residue was diluted with water and extracted with ethyl acetate. The extract was washed with water, dried over anhydrous sodium sulfate, filtered, and evaporated to dryness. Chromatography on silica gel with ethyl acetate–dichloromethane (2:1) as the eluent yielded **4** (2.62 g, 55%) as a black oil. $^1$H NMR (300 MHz; $CDCl_3$; $Me_4Si$) $\delta$ 1.27 (6H, t, $J = 7$ Hz, $2 \times CH_3$), 1.51 (3H, t, $J = 7$ Hz, $CH_3$), 2.07 (1H, br s, NH), 3.72 (4H, m, $2 \times CH_2$), 4.54 (2H, q, $J = 7$ Hz, $CH_2$), 6.11 (1H, s, CH), 7.22 [1H, dd, $J = 5$ and 8 Hz, C(5)H], 8.30 [1H, d, $J = 8$ Hz, C(4)H], 8.52 [1H, dd, $J = 1$ and 5 Hz, C(6)H]. FAB-MS $m/z$ 293 [$M^+ + 1$], $C_{15}H_{20}N_2O_4$ requires 292.33.

**4-Azaindole-2-carbaldehyde diethylacetal (5).** To a solution of sodium (0.11 g) in dry ethanol (20 cm$^3$) was added **4** (2.62 g, 8.97 mmol), and the mixture was stirred at 100 °C for 24 h. After removal of ethanol, the residue was diluted with water and extracted with ethyl acetate. The extract was washed with water, dried over anhydrous sodium sulfate, filtered, and evaporated to dryness. Chromatography on silica gel with ethyl acetate as the eluent yielded **5** as a light brown powder (1.03 g, 52%). Mp 110–115 °C; Anal. found: C, 65.28; H, 7.62; N, 12.71. $C_{12}H_{16}N_2O_2$ requires: C, 65.43; H, 7.32; N, 12.72%. $^1$H NMR (300 MHz; $CDCl_3$; $Me_4Si$) $\delta$ 1.27 (6H, t, $J = 7$ Hz, $2 \times CH_3$), 3.66 (4H, m, $2 \times CH_2$), 5.80 (1H, s, CH), 6.73 [1H, s, C(3)H], 7.10 [1H, dd, $J = 5$ and 8 Hz, C(6)H], 7.66 [1H, d, $J = 8$ Hz, C(7)H], 8.45 [1H, dd, $J = 1$ and 5 Hz, C(5)H], 8.59 (1H, br s, NH). FAB-MS $m/z$ 221 [$M^+ + 1$], $C_{12}H_{16}N_2O_2$ requires 220.27.

**4-Azaindole-2-carbaldehyde (6).** A solution of **5** (1.00 g, 4.54 mmol) in 1 M sulfuric acid (25 cm$^3$) was refluxed at 100 °C for 15 min. After the solution had cooled down to room temperature, the pH was adjusted to 10 with aqueous sodium sulfate solution. The precipitate was filtered off, washed with water, and dried under vacuum to yield **6** (0.46 g, 70%) as a red brown powder. Mp 219–222 °C (ref. 25 mp 210–212 °C). Anal. found: C, 65.39; H, 4.13; N, 19.19. $C_8H_6N_2O$ requires C, 65.75; H, 4.14; N, 19.17%. $^1$H NMR (300 MHz; $CDCl_3$; $Me_4Si$) $\delta$ 7.33 [1H, dd, $J = 5$ and 9 Hz, C(6)H], 7.49 [1H, s, C(3)H], 7.81 [1H, dd, $J = 1$ and 9 Hz, C(7)H], 8.63 [1H, dd, $J = 1$ and 5 Hz, C(5)H], 9.23 (1H, br s, NH), 9.98 (1H, s, CHO). FAB-MS $m/z$ 147 [$M^+ + 1$], $C_8H_6N_2O$ requires 146.15.

**2-(4-Azaindol-2-yl)-4,4,5,5-tetramethyl-4,5-dihydro-1*H*-imidazoline-1-oxyl-3-oxide (2).** To a solution of **6** (0.50 g, 3.42 mmol) in dry methanol (50 cm$^3$) was added 2,3-bis(hydroxyamino)-2,3-dimethylbutane (0.76 g, 5.13 mmol). The mixture was refluxed at 80 °C until the solids were dissolved completely, and then stirred at room temperature for 24 h. After the solvent was removed under vacuum, the residue was taken up in dichloromethane (200 cm$^3$), cooled to 0 °C, and then sodium periodide (4.39 g, 20.52 mmol) in water (200 cm$^3$) was added with stirring. The organic layer was washed with

water, dried over anhydrous sodium sulfate, filtered, and evaporated to dryness. Chromatography on silica gel with ethyl acetate–*n*-hexane (2:1) as the eluent yielded **2** (0.67 g, 72%), which was recrystallised as a dark blue block crystal by slow evaporation from a methanol solution. Mp 191–193 °C (decomp). Anal. found: C, 61.22; H, 6.30; N, 20.35. $C_{14}H_{17}N_4O_2$ requires C, 61.52; H, 6.27; N, 20.50%. FAB-MS $m/z$ 274 $[M^+ + 1]$, $C_{14}H_{17}N_4O_2$ requires 273.31.

### X-Ray diffraction analysis

A dark-blue needle crystal of **2** ($0.70 \times 0.30 \times 0.25$ mm) was measured at 297 K on a Rigaku four-circle AFC-7R diffractometer with graphite monochromated Mo-K$\alpha$ radiation ($\lambda = 0.71073$ Å). The data were collected using the $\omega$ scan technique to a maximum $2\theta$ value of 55.0°. The structure was solved by direct methods (SIR92[26]) and refined by SHELXL-97[27] on a Silicon graphics $O^2$ workstation with the program system teXsan.[28] Three standard reflections were measured every 150 reflections. An absorption correction was made by the $\Psi$ scan method. The positions of all hydrogen atoms were introduced by difference Fourier maps. Non-hydrogen atoms were treated anisotropically and hydrogen atoms were treated isotropically. Crystal data are summarized in Table 2.

CCDC reference number 202379. See http://www.rsc.org/suppdata/nj/b2/b210820h/ for crystallographic files in CIF or other electronic format.



## Acknowledgements

We wish to thank Prof. S. Yabushita at Keio University for his helpful discussions about DFT calculations and Dr. M. Tsuchimoto at Keio University for his helpful discussions about X-ray analysis. H. N. thanks Keio University (Keio Leading-edge Laboratory of Science & Technology) for financial support.

## References

1 O. Kahn, *Molecular Magnetism*, VCH, Weinheim, 1993; *Magnetic Properties of Organic Radicals*, ed. P. M. Lahti, Marcel Dekker, New York, 1999; *Magnetism: Molecules to Materials*, eds. J. S. Miller and M. Drillon, VCH, Weinheim, 2001.
2 M. Tamura, Y. Nakazawa, D. Shiomi, K. Nozawa, Y. Hosokoshi, M. Ishikawa, M. Takahashi and M. Kinoshita, *Chem. Phys. Lett.*, 1991, **186**, 401.
3 R. Chiarelli, M. A. Novak, A. Rassat and J. L. Tholence, *Nature*, 1993, **363**, 147.
4 A. J. Banister, N. Bricklebank, I. Lavender, J. M. Rawson, C. I. Gregory, B. K. Tanner, W. Clegg, M. R. J. Elsegood and F. Palacio, *Angew. Chem., Int. Ed. Engl.*, 1996, **35**, 2533.
5 G. R. Desiraju, *Chem. Commun.*, 1997, 1475.
6 T. Sugawara, M. M. Matsushita, A. Izuoka, N. Wada, N. Takeda and M. Ishikawa, *J. Chem. Soc., Chem. Commun.*, 1994, 1723; J. Cirujeda, M. Mas, E. Molins, F. L. Panthou, J. Laugier, J. G. Park, C. Paulsen, P. Rey, C. Rovira and J. Veciana, *J. Chem. Soc., Chem. Commun.*, 1995, 709.
7 A. Lang, Y. Pei, L. Ouahab and O. Kahn, *Adv. Mater.*, 1996, **8**, 60.
8 F. L. Panthou, D. Luneau, J. Laugier and P. Rey, *J. Am. Chem. Soc.*, 1993, **115**, 9095.
9 (*a*) N. Yoshioka, M. Irisawa, Y. Mochizuki, T. Kato, H. Inoue and S. Ohba, *Chem. Lett.*, 1997, 251; (*b*) H. Nagashima, M. Irisawa, N. Yoshioka and H. Inoue, *Mol. Cryst. Liq. Cryst.*, 2002, **376**, 371; (*c*) H. Nagashima, H. Inoue and N. Yoshioka, *Synth. Met.* in press.
10 H. M. McConnell, *J. Chem. Phys.*, 1963, **39**, 1910.
11 T. Sakamoto, Y. Kondo, S. Iwashita and H. Yamanaka, *Chem. Pharm. Bull.*, 1987, **35**, 1823 and references cited therein.
12 E. F. Ullman, J. H. Osiechi, D. G. B. Boocock and R. Darcy, *J. Am. Chem. Soc.*, 1972, **94**, 7049.
13 The EPR spectrum simulation was carried out using PEST WinSIM: D. Duling, National Institute of Environmental Health Sciences, Research Triangle Park, NC, USA, 1996.
14 J. Cirujeda, J. Vidal-Gancedo, O. Jürgens, F. Mota, J. J. Novoa, C. Rovira and J. Veciana, *J. Am. Chem. Soc.*, 2000, **122**, 11 393.
15 M. J. Frisch, G. W. Trucks, H. B. Schlegel, G. E. Scuseria, M. A. Robb, J. R. Cheeseman, V. G. Zakrzewski, J. A. Montgomery, Jr., R. E. Stratmann, J. C. Burant, S. Dapprich, J. M. Millam, A. D. Daniels, K. N. Kudin, M. C. Strain, O. Farkas, J. Tomasi, V. Barone, M. Cossi, R. Cammi, B. Mennucci, C. Pomelli, C. Adamo, S. Clifford, J. Ochterski, G. A. Petersson, P. Y. Ayala, Q. Cui, K. Morokuma, D. K. Malick, A. D. Rabuck, K. Raghavachari, J. B. Foresman, J. Cioslowski, J. V. Ortiz, A. G. Baboul, B. B. Stefanov, G. Liu, A. Liashenko, P. Piskorz, I. Komaromi, R. Gomperts, R. L. Martin, D. J. Fox, T. Keith, M. A. Al-Laham, C. Y. Peng, A. Nanayakkara, C. Gonzalez, M. Challacombe, P. M. W. Gill, B. G. Johnson, W. Chen, M. W. Wong, J. L. Andres, M. Head-Gordon, E. S. Replogle and J. A. Pople, Gaussian 98, Rev. A.9Gaussian, Inc., Pittsburgh, PA, USA, 1998.
16 A. D. Becke, *Phys. Rev. A*, 1988, **38**, 3098; C. Lee, W. Yang and R. G. Parr, *Phys. Rev. B*, 1988, **37**, 785; A. D. Becke, *J. Chem. Phys.*, 1993, **98**, 5648.
17 V. Barone, in *Recent Advances in Density Functional Methods, Part I*, ed. D. P. Chong, World Scientific Publishing Co., Singapore, 1996, p. 287.
18 D. E. Woon and T. H. Dunning Jr., *J. Chem. Phys.*, 1993, **98**, 1358.
19 R. R. Gupta, in *Lanbort-Börnstein, Neue Series II/16*, eds. K.-H. Hellwege and A.M. Hellwege, Springer-Verlag, Berlin, 1986, p. 4.
20 B. Bleaney and K. D. Bowers, *Proc. R. Soc. London, Ser. A*, 1952, 214.
21 S. Yamanaka, T. Kawakami, H. Nagao and K. Yamaguchi, *Chem. Phys. Lett.*, 1994, **231**, 25.
22 Y. Hosokoshi, M. Tamura, D. Shiomi, N. Iwasawa, K. Nozawa, M. Kinoshita, H. A. Katori and T. Goto, *Physica B*, 1994, **201**, 497.
23 B. Esat, P. M. Lahti, M. Julier and F. Palacio, *CrystEngComm*, 2002, **11**, 59.
24 M. Lamchen and T. W. Mittag, *J. Chem. Soc. (C)*, 1966, 2300.
25 B. Frydman, S. J. Reil, J. Boned and H. Rapoport, *J. Org. Chem.*, 1968, **33**, 3762.
26 A. Altomare, M. C. Burla, M. Camalli, M. Cascarano, C. Giacovazzo, A. Guagliardi and G. Polidori, *J. Appl. Crystallogr.*, 1994, **27**, 435.
27 G. M. Sheldrich, SHELXL-97: Program for the Refinement of Crystal Structures, University of Göttingen, Germany, 1997.
28 teXsan, v. 1.11, Single Crystal Structure Analysis Software, MSC, The Woodlands, TX, US and Rigaku, Tokyo, Japan, 1999.